

## Statistical analysis

All data in the tables and figures are expressed as the mean  $\pm$  standard error of the mean (SEM). Statistical analysis was carried out using Static Analysis System (SAS) software. The significance of difference was determined using the Dunnett multiple test (in the intermittent treatment group or the continuous treatment group for comparison between C-CON and C40-PTH or C280-PTH) and the Student's *t* test (in the continuous treatment group for comparison between C-CON and C40-PTH or in the continuous-withdrawal treatment group). A *p* value of  $<0.05$  was considered significant.

## Results

## Effects of various PTH treatment regimens on serum calcium

Because a critical adverse effect of PTH treatment is the induction of hypercalcemia, we first determined the appropriate PTH-treatment regimens that do not induce hypercalcemic action. As shown in Fig. 1, intermittent PTH injections both once a week (I $\times$ 1-PTH) and 3 times a week (I $\times$ 3-PTH) did not induce any increase in serum calcium levels, as compared with those of control rats (I-CON). In contrast, continuous PTH treatment with a high dose of PTH (280  $\mu$ g/kg/week; C280-PTH) significantly increased the serum calcium levels from day 1 to day 7 during the treatment, resulting in hypercalcemia (defined as a serum calcium level greater than 10.5 mg/dl). Continuous PTH treatment with a dose of 40  $\mu$ g/kg/week (C40-PTH) transiently increased the serum calcium level only on day 2, as compared with that in control rats, though it was within the normocalcemic range (8.4–10.4 mg/dl). Similarly, continuous PTH treatment for 24 h followed by withdrawal of PTH treatment for 6 days (PTH-WD) increased the serum calcium level only on day 1, but this level was also within the normocalcemic range. Thus, among the PTH treatment regimens described above, a high-dose continuous PTH treatment (C280-PTH) induced apparent hypercalcemia during PTH treatment. We therefore excluded this group from further investigations of bone status.

## Effects of various PTH treatment regimens on BMD

Table 2 summarizes the BMD of the entire femur and the proximal, diaphyseal, and distal parts of the femur. Intermittent PTH treatment for 4 weeks with 1 injection per week (I $\times$ 1-PTH) produced no significant differences in the BMD at each part of the bones measured, but the intermittent PTH treatment for the same period with 3 injections

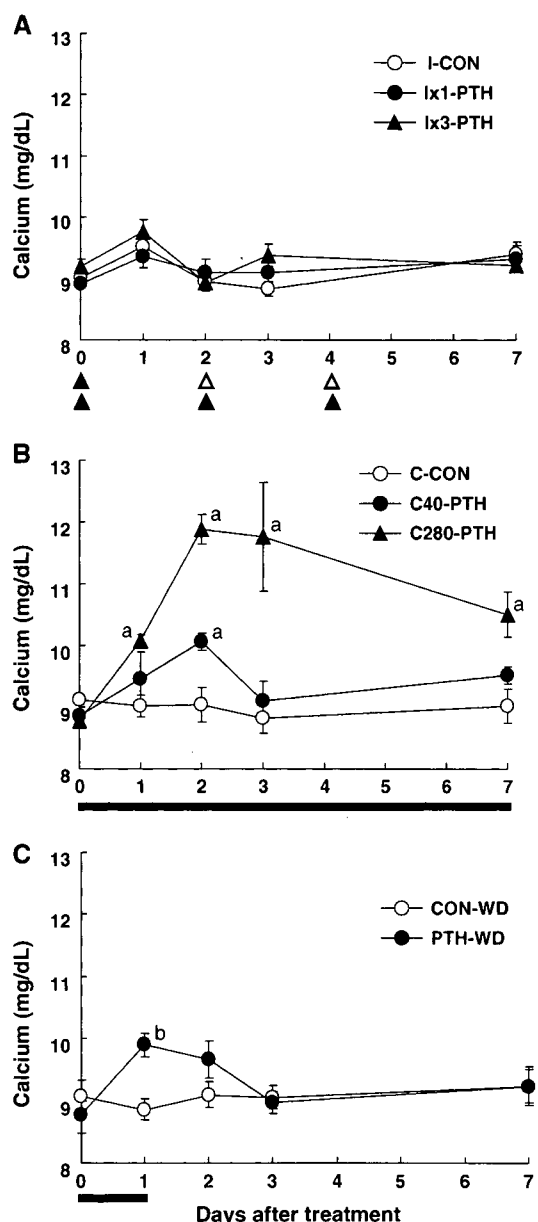


**Fig. 1** Serum total calcium in rats treated with intermittent PTH (a), continuous PTH (b), and continuous PTH withdrawal (c). a Solid triangles indicate the days of PTH injections, and open triangles indicate the days of vehicle injections. b, c The treatment periods are indicated as black bars. Values are represented as mean  $\pm$  SEM ( $n = 5$ ). <sup>a</sup> $p < 0.05$  vs. C-CON, <sup>b</sup> $p < 0.05$  vs. CON-WD

per week (I $\times$ 3-PTH) significantly increased the BMD of the entire femur and the diaphyseal and distal parts of the femur, as compared with that in the corresponding control rats (I-CON). Continuous treatment with PTH (C40-PTH) for 4 weeks significantly decreased the BMD of the entire femur and the proximal region of the femur, as compared with that in the corresponding control rats (C-CON). In contrast, repetitive treatments for 4 weeks with continuous PTH infusion for 24 h followed by withdrawal for 6 days (PTH-WD) significantly increased the BMD in the

**Table 2** Bone mineral density of femurs in rats treated with various PTH treatment protocols

	Whole (mg/cm <sup>2</sup> )	Proximal (mg/cm <sup>2</sup> )	Diaphysis (mg/cm <sup>2</sup> )	Distal (mg/cm <sup>2</sup> )
I-CON	114.4 ± 1.4	113.8 ± 1.8	105.4 ± 1.5	123.0 ± 1.2
I×1-PTH	118.6 ± 1.7	116.1 ± 1.8	109.8 ± 2.3	128.7 ± 2.2
I×3-PTH	121.7 ± 2.6 <sup>a</sup>	119.2 ± 2.7	112.3 ± 1.8 <sup>a</sup>	131.9 ± 3.4 <sup>a</sup>
C-CON	117.5 ± 1.2	117.2 ± 1.1	109.7 ± 1.9	128.4 ± 3.8
C40-PTH	112.1 ± 1.4 <sup>b</sup>	110.8 ± 1.5 <sup>b</sup>	104.5 ± 2.1	119.9 ± 1.9
CON-WD	114.4 ± 2.0	111.9 ± 1.5	106.4 ± 1.3	123.4 ± 3.4
PTH-WD	118.4 ± 1.5	118.7 ± 1.7 <sup>c</sup>	109.2 ± 1.7	126.2 ± 1.5

Values are expressed as mean ± SEM (n = 6). Comparisons of data were performed using Dunnett's test (I-CON, I×1-PTH, and I×3-PTH) and the unpaired t test (C-CON and C40-PTH; CON-WD and PTH-WD)

Significance is indicated by: <sup>a</sup>p < 0.05, I×3-PTH vs. I-CON; <sup>b</sup>p < 0.05, C40-PTH vs. C-CON; and <sup>c</sup>p < 0.05 PTH-WD vs. CON-WD group

proximal region by 6.0%, as compared with that in the control group (CON-WD).

μCT analysis of cortical bone

Both intermittent PTH treatments, i.e., I×1-PTH and I×3-PTH, slightly increased the cortical thickness, but this increase was not significantly different from that observed in the control group (I-CON; Fig. 2). C40-PTH induced no apparent changes in cortical thickness, as compared with those in the control rats (C-CON; Fig. 2). PTH-WD significantly increased the cortical thickness, as compared with that in the control group (CON-WD; Fig. 2).

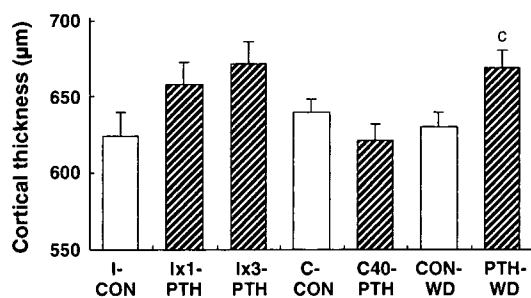
Bone histomorphometric analyses for cancellous bone

Figure 3 summarizes the results of bone histomorphometric analyses at the metaphyseal region of the proximal tibiae. I×1-PTH induced no significant differences in any parameter, as compared with those in the control rats (I-CON). However, I×3-PTH increased the values of BV/TV, Tb.Th, Ob.S/BS, and BFR/BS, as compared with those in the control rats (I-CON). C40-PTH increased the osteoclast number (N.Oc/BS), but produced no significant differences in the other parameters. PTH-WD significantly increased

the OV/BV, Tb.Th, Ob.S/BS, and BFR/BS, as compared with those in the control rats (CON-WD). In the PTH-WD group, a slight but significant decrease in the trabecular number (Tb.N) was also observed. No apparent increase in the N.Oc/BS was observed in this group. We found no significant differences on mineralization lag time (Mlt: O.Th/MAR × OS/MS) among each group (Fig. 3). These data indicate that PTH-WD treatment produces anabolic effects on trabecular bones by stimulating bone formation, without the continuously elevated osteoclastic bone resorption observed in the C40-PTH treatment.

Mechanical properties of the femoral neck

Table 3 summarizes the mechanical properties of the femoral neck in rats treated with various regimens. I×3-PTH and PTH-WD slightly increased the maximum load, but these values were not significantly different from those in the control rats. The stiffness of the femoral neck tended to be less in the C40-PTH and PTH-WD treatment groups than in each control group. PTH-WD treatment increased the energy required to fracture by 47%, but this value was not significantly different from the values of the control femurs.



**Fig. 2** Cortical thickness of femoral diaphyses measured by micro-CT, as described in "Materials and methods." Values are presented as mean ± SEM (n = 6). <sup>c</sup>p < 0.05 vs. CON-WD

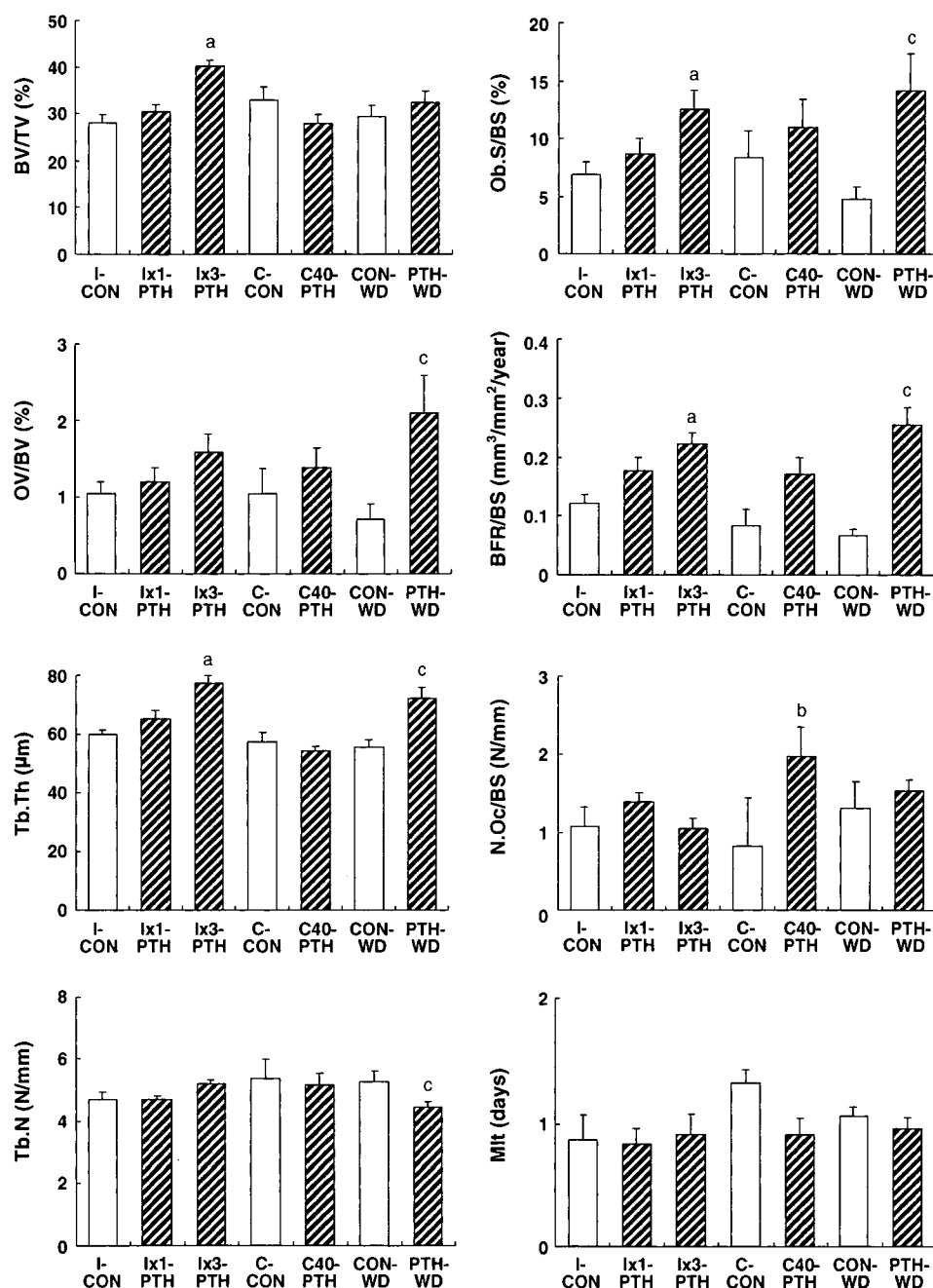
Discussion

Various animal experiments have shown that in rats, a continuous infusion of PTH induced catabolic actions in bones, resulting in decreased bone mass and hypercalcemia. However, intermittent treatment with PTH exerted anabolic effects by increasing the bone mass in intact and ovariectomized (OVX) rats and humans [4, 6, 8]. Previous pharmacokinetic studies have indicated that the duration of the serum concentration of PTH above the baseline level of endogenous PTH is a critical factor in regulating such catabolic and anabolic actions on the bone mass [6, 13].

**Fig. 3** Histomorphometric indices of trabecular bone in the proximal metaphyses of tibiae in rats treated with various administration regimens for 4 weeks, as described in "Materials and methods".

I-CON, intermittent treatment control; Ix1-PTH, intermittent injection of PTH once a week; Ix3-PTH, intermittent injections of PTH 3 times a week; C-CON, continuous treatment control; C40-PTH, continuous infusion of PTH for 4 weeks; CON-WD, control for PTH continuous treatment followed by PTH withdrawal; PTH-WD, continuous infusion of PTH for 24 h followed by PTH withdrawal for 6 days.

Values are presented as mean  $\pm$  SEM ( $n = 6$ ). <sup>a</sup> $p < 0.05$  vs. I-CON, <sup>b</sup> $p < 0.05$  vs. C-CON, <sup>c</sup> $p < 0.05$  vs. CON-WD



Sustained serum concentration of PTH above the baseline level for more than 6 h per day causes catabolic effects such as decreased bone mass and hypercalcemia; these effects are symptoms of hyperparathyroidism [5, 14]. We showed that the repetition of a continuous infusion of PTH for 24 h followed by a 6-day withdrawal period (PTH-WD) induced some anabolic activity in the bone metabolism, without causing hypercalcemia. This PTH treatment may increase the serum PTH level for more than 6 h on the day of infusion; therefore, a substantial period of withdrawal is important to induce the anabolic effects of PTH in bone

metabolism, regardless of continuous treatment with PTH for 24 h. Interestingly, Ishii et al. [15] reported that intermittent lowering of the serum PTH level exerted "anabolic-like" effects on bone mass in rats with chronic renal insufficiency. In their study, intermittent lowering of the serum PTH level increased the trabecular bone thickness, but not the trabecular number; this finding is similar to that observed in the rats of the PTH-WD group in our study. Another study reported that a continuous PTH infusion for 7 days followed by a 21 day withdrawal period increased the mechanical properties of bones [16]; however, the dose

**Table 3** Mechanical properties of the femoral head in rats treated with various treatment protocols of PTH for 28 days

	Femoral head compression		
	Maximum load (N)	Stiffness (N/mm)	Energy to fracture (N mm)
I-CON	86.7 ± 5.5	264 ± 27	19.0 ± 2.4
I×1-PTH	82.9 ± 5.0	194 ± 28	23.4 ± 3.6
I×3-PTH	96.8 ± 2.8	304 ± 38	21.0 ± 3.4
C-CON	85.1 ± 5.7	205 ± 13	17.0 ± 3.0
C40-PTH	73.6 ± 3.1	176 ± 23	19.8 ± 2.7
CON-WD	81.2 ± 8.0	273 ± 36	21.4 ± 5.8
PTH-WD	96.1 ± 7.3	172 ± 32	31.3 ± 4.4

Values are expressed as mean ± SEM ( $n = 6$ ). No significance was detected

used in this study (40 µg/kg/day for 7 days) caused transitional hypercalcemia in our experiment (Fig. 1). These results indicate that suitable periods of sustained serum PTH level and PTH withdrawal are important to induce the anabolic effects of PTH on bone, even after continuous PTH treatment.

Our study showed that 4 cycles of PTH-WD treatment as well as I×3-PTH treatment induced some anabolic activity in the bone metabolism. Both treatments increased Tb.Th, Ob.S/BS, and BFR/BS. However, these 2 regimens also produced some other effects. PTH-WD treatment significantly increased the OV/BV, but I×3-PTH treatment failed to significantly increase it. In contrast, PTH-WD treatment failed to increase BV/TV, and I×3-PTH treatment significantly increased it. The Tb.N was maintained in the I×3-PTH group at the level of the control group, but the Tb.N was reduced in the PTH-WD group. This decrease in the Tb.N in the PTH-WD group may be a cause of the non-elevated values of BV/TV, which was observed in the I×3-PTH group. Further, the dissociation between increased Tb.Th and decreased Tb.N in the PTH-WD group will provide important information to understand the action mechanism of PTH-WD treatment. We speculate that the decreased Tb.N might be due to transient or acute bone resorption during continuous PTH treatment for the initial 24 h, though N.Oc/BS was not significantly increased at the end of PTH-WD treatment. Thereafter, active bone formation occurred, and it contributed the increased Tb.Th. Thus, anabolic actions induced by the PTH-WD treatment on the bone structure seem to be different from those observed in the intermittent PTH treatment group without changes in mineralization lag time.

Cortical bone thickness is an important factor that determines the mechanical characteristics of a femur and predicts the bone strength and fracture risk in patients with osteoporosis [17]. Although PTH-WD treatment increased the cortical thickness, the PTH-WD group had mild

increases in ultimate force at maximal load without significant differences as well as the I×3-PTH group. The PTH-WD group showed the increase in energy to fracture, but it was not significantly different from other groups. Since PTH-WD treatment failed to induce significant changes in the mechanical properties, it is necessary to conduct long-term studies for more than 4 weeks to record apparent improvements in the mechanical properties.

Continuous PTH treatment as well as intermittent PTH treatment stimulates bone formation, but the former treatment enhances osteoclastic bone resorption that exceeds the stimulated bone formation. In the present study, PTH-WD treatment as well as I×3-PTH treatment prevented increases in the N.Oc/BS, whereas prolonged continuous PTH treatment for 7 days (C40-PTH) significantly increased the N.Oc/BS. These results suggest that a suitable PTH withdrawal period contributes to the induction of anabolic bone action by preventing overstimulation of osteoclastic bone resorption. This assumption is supported by studies that showed that the ratio of the receptor activator of the nuclear factor κB ligand (RANKL) to osteoprotegerin (OPG) (RANKL/OPG ratio) and MCP-1 expression, which are known to be the key regulators of osteoclast differentiation, depend on the exposure time to PTH [18, 19].

The recommended regimen of recombinant human PTH(1-34), Forteo, which is a potent FDA-approved drug for the treatment of osteoporosis, is once a day by self-administered injections. The compliance of patients with this treatment is moderate because of high cost and adverse effects such as pain at the injection site [9, 20, 21]. To overcome these problems, several researchers have attempted the use of less- or noninvasive and inexpensive delivery systems for PTH [11, 22, 23], including an injectable formulation with a low frequency of injection and an oral delivery system. Balck et al. [24] showed that daily injections of PTH (1–84) for a month followed by weekly injections of PTH (1–84) for 11 months increased the vertebral BMD in patients with osteoporosis; this suggests that less frequent PTH injections can be used as an anabolic therapeutic regimen. One of the hurdles in oral administration appears to be the attainment of pulsatile PTH plasma concentrations, which induce anabolic effects in the bone. In the present study, we showed that the repetition of 24-h continuous infusions of PTH followed by 6-day withdrawal periods induced anabolic effects in the bone. Another critical issue that should be considered carefully is the induction of hypercalcemia by PTH administration. Horwitz et al. [25] revealed that continuous infusion of PTH for 23 h did not induce severe hypercalcemia in healthy human volunteers. Our results indicated that continuous PTH infusion for 24 h slightly increased the serum calcium level, which remained lower than the

hypercalcemic level on day 1, and the normocalcemic level was regained from day 2. Since the serum calcium level after the oral administration of PTH will return to normal level within 24 h, oral administration followed by PTH withdrawal will be a potential therapeutic regimen of PTH treatment that can induce anabolic effects in the bone without inducing hypercalcemia.

It is essential to determine the suitable intervals of PTH exposure and withdrawal in order to establish a therapeutic regimen for PTH treatment. Katz et al. [26] reported that in 9- to 13-week-old male rats, the resorption and formation periods are 2.1 days and 14.4 days, respectively, and these periods are prolonged in older rats and humans; therefore, the bone turnover period, expressed as the activation frequency or bone remodeling unit, is a critical factor in determining suitable treatment periods. In addition, this study raised the possibility that variable regimens of PTH treatment regulate osteoclastic bone resorption and osteoblastic bone formation. Further studies on the doses of PTH and the durations of PTH exposure and withdrawal are required to determine a suitable regimen that induces more effective anabolic action of PTH on the bone structure. Since a recent study demonstrated that PTH predominantly affected preosteoblastic proliferation rather than osteoblastic bone synthesis, the effects of PTH-WD treatment on proliferation of preosteoblastic cells will be of particular interest for understanding the mechanism underlying such PTH treatment [27].

**Acknowledgments** We thank Dr. Toshinori Ishizuya for his instructive and helpful suggestions. This work was supported in part by a Grant-in-Aid for Scientific Research from the Japan Society for the Promotion of Science (14104015 to A.Y.) and by a grant from the Japanese Ministry of Education, Global Center of Excellence (GCOE) Program, "International Research Center for Molecular Science in Tooth and Bone Diseases."

## References

- Uzawa T, Hori M, Ejiri S, Ozawa H (1995) Comparison of the effects of intermittent and continuous administration of human parathyroid hormone (1–34) on rat bone. *Bone* 16:477–484
- Iida-Klein A, Lu SS, Kapadia R, Burkhart M, Moreno A, Dempster DW, Lindsay R (2005) Short-term continuous infusion of human parathyroid hormone 1–34 fragment is catabolic with decreased trabecular connectivity density accompanied by hypercalcemia in C57BL/J6 mice. *J Endocrinol* 186:549–557
- Dempster DW, Cosman F, Kurland ES, Zhou H, Nieves J, Wolfert L, Shane E, Plavetic K, Muller R, Bilezikian J, Lindsay R (2001) Effects of daily treatment with parathyroid hormone on bone microarchitecture and turnover in patients with osteoporosis: a paired biopsy study. *J Bone Miner Res* 16:1846–1853
- Ejersted C, Andreassen TT, Oxlund H, Jorgensen PH, Bak B, Haggblad J, Torring O, Nilsson MH (1993) Human parathyroid hormone (1–34) and (1–84) increase the mechanical strength and thickness of cortical bone in rats. *J Bone Miner Res* 8:1097–1101
- Dobnig H, Turner RT (1997) The effects of programmed administration of human parathyroid hormone fragment (1–34) on bone histomorphometry and serum chemistry in rats. *Endocrinology* 138:4607–4612
- Hock JM, Gera I, Fonseca J, Raisz LG (1988) Human parathyroid hormone-(1–34) increases bone mass in ovariectomized and orchidectomized rats. *Endocrinology* 122:2899–2904
- Riond JL, Goliat-von Fischer I, Kuffer B, Toromanoff A, Forrer R (1998) Influence of the dosing frequency of parathyroid hormone-(1–38) on its anabolic effect in bone and on the balance of calcium, phosphorus and magnesium. *Z Ernahrungswiss* 37:183–189
- Neer RM, Arnaud CD, Zanchetta JR, Prince R, Gaich GA, Reginster JY, Hodsman AB, Eriksen EF, Ish-Shalom S, Genant HK, Wang O, Mitlak BH (2001) Effect of parathyroid hormone (1–34) on fractures and bone mineral density in postmenopausal women with osteoporosis. *N Engl J Med* 344:1434–1441
- Taylor K, Gold DT, Miller P, Chen P, Wong M, Krohn K (2008) Teriparatide therapy in a community setting: persistence and use of other osteoporosis medications in DANCE. ASBMR meeting 2008 abstract 2008:Sa395
- Kawase M, Tsuda M (1994) Vitamin D independent anabolic action of PTH in vivo. *J Bone Miner Metab* 12:S27–S31
- Hoyer H, Perera G, Bernkop-Schnurch A (2010) Noninvasive delivery systems for peptides and proteins in osteoporosis therapy: a retrospective. *Drug Dev Ind Pharm* 36:31–44
- Ke HZ, Shen VW, Qi H, Crawford DT, Wu DD, Liang XG, Chidsey-Frink KL, Pirie CM, Simmons HA, Thompson DD (1998) Prostaglandin E2 increases bone strength in intact rats and in ovariectomized rats with established osteopenia. *Bone* 23:249–255
- Parfitt AM, Drezner MK, Glorieux FH, Kanis JA, Malluche H, Meunier PJ, Ott SM, Recker RR (1987) Bone histomorphometry: standardization of nomenclature, symbols, and units. Report of the ASBMR Histomorphometry Nomenclature Committee. *J Bone Miner Res* 2:595–610
- Frolik CA, Black EC, Cain RL, Satterwhite JH, Brown-Augsburger PL, Sato M, Hock JM (2003) Anabolic and catabolic bone effects of human parathyroid hormone (1–34) are predicted by duration of hormone exposure. *Bone* 33:372–379
- Ishii H, Wada M, Furuya Y, Nagano N, Nemeth EF, Fox J (2000) Daily intermittent decreases in serum levels of parathyroid hormone have an anabolic-like action on the bones of uremic rats with low-turnover bone and osteomalacia. *Bone* 26:175–182
- Lotinun S, Evans GL, Bronk JT, Bolander ME, Wronski TJ, Ritman EL, Turner RT (2004) Continuous parathyroid hormone induces cortical porosity in the rat: effects on bone turnover and mechanical properties. *J Bone Miner Res* 19:1165–1171
- Cheng X, Li J, Lu Y, Keyak J, Lang T (2007) Proximal femoral density and geometry measurements by quantitative computed tomography: association with hip fracture. *Bone* 40:169–174
- Ma YL, Cain RL, Halladay DL, Yang X, Zeng Q, Miles RR, Chandrasekhar S, Martin TJ, Onyia JE (2001) Catabolic effects of continuous human PTH (1–38) in vivo is associated with sustained stimulation of RANKL and inhibition of osteoprotegerin and gene-associated bone formation. *Endocrinology* 142:4047–4054
- Li X, Qin L, Bergenstock M, Bevelock LM, Novack DV, Partridge NC (2007) Parathyroid hormone stimulates osteoblastic expression of MCP-1 to recruit and increase the fusion of pre-osteoclasts. *J Biol Chem* 282:33098–33106
- Gold DT, Weinstein D, Pohl G, Chen Y, Krohn K, Meadows E (2009) Factors associated with discontinuation of teriparatide treatment: One-year results from the DANCE observational study addendum. ASBMR meeting 2009 abstract 2009:MO0357

21. Miller PD, Silverman SL, Gold DT, Taylor KA, Chen P, Wagman RB (2006) Rationale, objectives and design of the Direct Analysis of Nonvertebral Fracture in the Community Experience (DANCE) study. *Osteoporos Int* 17:85–90
22. Suzuki Y, Nagase Y, Iga K, Kawase M, Oka M, Yanai S, Matsumoto Y, Nakagawa S, Fukuda T, Adachi H, Higo N, Ogawa Y (2002) Prevention of bone loss in ovariectomized rats by pulsatile transdermal iontophoretic administration of human PTH(1–34). *J Pharm Sci* 91:350–361
23. Morley P (2005) Delivery of parathyroid hormone for the treatment of osteoporosis. *Expert Opin Drug Deliv* 2:993–1002
24. Black DM, Bouxsein ML, Palermo L, McGowan JA, Newitt DC, Rosen E, Majumdar S, Rosen CJ (2008) Randomized trial of once-weekly parathyroid hormone (1–84) on bone mineral density and remodeling. *J Clin Endocrinol Metab* 93:2166–2172
25. Horwitz MJ, Tedesco MB, Sereika SM, Syed MA, Garcia-Ocaña A, Bisello A, Hollis BW, Rosen CJ, Wysolmerski JJ, Dann P, Gundberg C, Stewart AF (2005) Continuous PTH and PTHrP infusion causes suppression of bone formation and discordant effects on 1, 25(OH)<sub>2</sub> vitamin D. *J Bone Miner Res* 20:1792–1803
26. Katz I, Li M, Joffe I, Stein B, Jacobs T, Liang XG, Ke HZ, Jee W, Epstein S (1994) Influence of age on cyclosporin A-induced alterations in bone mineral metabolism in the rat in vivo. *J Bone Miner Res* 9:59–67
27. Luiz de Freitas PH, Li M, Ninomiya T, Nakamura M, Ubaidus S, Oda K, Udagawa N, Maeda T, Takagi R, Amizuka N (2009) Intermittent PTH administration stimulates pre-osteoblastic proliferation without leading to enhanced bone formation in osteoclast-less *c-fos*<sup>-/-</sup> mice. *J Bone Miner Res* 24:1586–1597

**Downregulation of keratin 4 and keratin 13 expression in oral squamous cell carcinoma and epithelial dysplasia: a clue for the histopathogenesis**

Running title: keratin 4 and keratin 13 in oral cancer

Kei Sakamoto,<sup>1</sup> Tadanobu Aragaki,<sup>2</sup> Kei-ichi Morita,<sup>3</sup> Hiroshi Kawachi,<sup>4</sup> Kou Kayamori,<sup>1</sup> Shoichi Nakanishi,<sup>1</sup> Ken Omura,<sup>3</sup> Yoshio Miki,<sup>5,6</sup> Norihiko Okada,<sup>7</sup> Ken-ichi Katsube,<sup>1</sup> Toichiro Takizawa<sup>8</sup> & Akira Yamaguchi<sup>1</sup>

Sections of <sup>1</sup>Oral Pathology, <sup>2</sup>Maxillofacial Surgery, <sup>3</sup>Oral and Maxillofacial Surgery, <sup>4</sup>Human Pathology, and <sup>7</sup>Diagnostic Oral Pathology, Graduate School, Tokyo Medical and Dental University, Tokyo Japan

<sup>5</sup>Section of Molecular Genetics, Medical Research Institute, Tokyo Medical and Dental University, Tokyo, Japan

<sup>6</sup>Department of Genetic Diagnosis, Cancer Institute, Japanese Foundation for Cancer Research, Tokyo, Japan

<sup>8</sup>Section of Molecular Pathophysiology, Graduate School of Allied Health Sciences, Tokyo Medical and Dental University, Tokyo, Japan

Corresponding author

Section of Oral Pathology, Tokyo Medical and Dental University, Yushima 1-5-45, Bunkyo-ku, Tokyo 113-0034, Japan

Tel.: +81 3 5803 5454; Fax: +81 3 5803 0188

E-mail address: s-kei.mpa@tmd.ac.jp

**Abstract**

*Aims:*

This study aimed to identify relevant keratin subtypes that may associate with the pathogenesis of oral epithelial neoplasms.

*Methods and results:*

Expression of all the keratin subtypes was examined by cDNA microarray analysis of 43 oral squamous cell carcinoma (OSCC) cases. Expression of the major keratins was further examined by immunohistochemical staining of 100 OSCC and oral epithelial dysplasia (OED) cases. Many changes in keratin expression were observed, and significantly, consistent downregulation of keratin 4 (K4) and K13 expression was also observed. Aberrant expression of K4 and K13 was associated with changes of the affected oral epithelial morphology. Experiments with cell cultures transfected with various keratin subtypes suggested that alterations in keratin subtype expression can cause changes in cellular properties such as shape and movement.

*Conclusions:*

Aberrant expression of K4 and K13, which are the dominant pair of differentiation-related keratins

in oral keratinocytes, indicates dysregulation of epithelial differentiation in OSCC and OED. Therefore, these keratins, especially K4, would be useful for pathological diagnosis. We propose that the aberrant expression of K4 and K13 and concomitant upregulation of the other keratins may be one of the causative factors for morphological alterations in the affected epithelium.

## KEYWORDS

oral mucosa, squamous cell carcinoma, epithelial dysplasia, keratin, keratin 4, keratin 13, cytokeratin

## Introduction

Keratin is an intermediate filament cytoskeletal protein. The human genome contains 54 genes encoding functional keratins, of which 37 encode epithelial keratins and 17 encode hair keratins. Keratins can be divided into acidic and basic types; both types are coexpressed during the differentiation of epithelial tissues and arranged in heterotypic pairs to form chains of laterally aligned coiled-coil structure.<sup>1</sup> Since the composition of keratin pairs varies depending on cell type, differentiation status and environment, the assessment of the distribution of different keratin subtypes can facilitate cell typing and identification. Moreover, keratin subtyping is useful for cancer diagnosis, since cancer cells often exhibit abnormal keratin expression profiles.<sup>1</sup> Several studies have indicated that some specific keratin subtypes were either downregulated or upregulated in oral squamous cell carcinoma (OSCC) and oral epithelial dysplasia (OED).<sup>2-17</sup> However, these studies have investigated limited numbers of selective keratin subtypes, and hence, the results of different studies are often conflicting; this is probably because of the variations in the experimental procedures used, including the use of antibodies. Furthermore, the correlation of each subtype and its significance in pathogenesis has not been fully assessed. In

order to understand the significance of keratin expression in OSCC and OED, an in-depth analysis of all the keratin subtypes is required.

In this study, we performed exhaustive keratin profiling to elucidate the comprehensive alterations in the expression of keratin subtypes in OSCC and OED. Many changes in keratin expression were observed, but the most remarkable feature observed in OSCC and OED was the downregulation of keratins 4 and 13 that might be of relevance to both pathogenesis and diagnosis of these lesions.

## Materials and methods

### Clinical specimens

The surgical specimens from 43 patients with OSCC were collected for microarray analysis. The primary sites of cancer were tongue (18), gingiva (16), oral floor (5), buccal mucosa (3) and palate (1). Written informed consent was obtained from all the patients, and all the experimental procedures were approved by the Tokyo Medical and Dental University ethics committee. In addition, 100 specimens of OSCC and OED that were large enough to be sufficiently informative and contained normal epithelium were collected from the archives of the Dental Hospital at Tokyo Medical and Dental University. Grading of OED was performed according to the generally accepted criteria.<sup>18</sup>



### cDNA microarray analysis

Cancer cells were isolated by laser capture microdissection. Squamous epithelial cells adjacent to OSCC were isolated from the specimens of 9 patients as a normal control. Microarray analyses were performed as described previously.<sup>19</sup>

### Immunostaining

Immunostaining was performed according to the standard protocol. For antigen retrieval, the sections were placed in TE buffer (10 mM Tris (pH = 9.0) and 1 mM EDTA) and autoclaved at 120 °C for 20 min. The primary antibodies used in this study were anti-K1 (N-20, Santa Cruz), K2e (Ks2.342.7.1, Progen), K4 (EP1599Y, Epitomics), K5 (XM26, Monosan), K6 (LHK6B, Neomarkers), K7 (RN7, Dako), K8 (TS1, Novocastra), K9 (Ks9.70/Ks9.216, EuroDiagnostica), K10 (DE-K10, Neomarkers), K13 (KS-1A3, Novocastra), K14 (LL002, Abcam), K15 (EPR1614Y, Epitomics), K16 (LL025, Neomarkers), K17 (E3, Dako), K18 (DC10, Dako), K19 (EP1580Y, Epitomics), K20 (PW1, Dako) and hair keratins (AE13, Santa Cruz). Anti-mouse IgG-Alexafluor 594, anti-rabbit IgG-Alexafluor 488 (Invitrogen), or Envision Dual link kit (Dako) was used as the secondary antibody. Evaluation of the expression was done by comparing the staining in the lesion with that in the normal epithelium of the same specimen.

### Molecular cloning of keratin genes

Human *K4* cDNA (IMAGE: 5453644) was purchased from Geneservice (Cambridge, UK). Human *K5*, *K13*, *K14* and *K17* cDNAs were synthesized by reverse

transcriptase-polymerase chain reaction of RNA obtained from the gingiva of a male volunteer. *K4* and *K5* were cloned into pAcGFP1-C2 (Clontech) and *K13*, *K14* and *K17* were cloned into pDsRed-Monomer-N1 (Clontech). *Dominant negative K4 (dnK4)*, lacking the carboxyl terminal region (from S414 to R594), was the deletion construct of *K4*. Details of the cloning procedures will be provided upon request.

### Cell culture

HEK293T, Ca9-22, and U2OS cells were cultured in Dulbecco's modified Eagle medium containing 10% fetal calf serum. Transfections were performed using FuGene6 (Roche Diagnostics). To assess the effect of different keratin expression on the cell motility, cells seeded in a Boyden chamber (pore size 8 µm, BD Falcon) were transfected with mock, *K13*, or *K17* plasmid, and cell movement assay was performed as previously described.<sup>20</sup>

## Results

### cDNA microarray analysis of OSCC

Expression level of the genes encoding each keratin subtype was represented as the mean of the signal intensities of OSCC samples and control samples (Figure 1A) and the ratios of the expression level in the OSCC samples to that in the control samples (Figure 1B). The genes with a low signal in Figure 1A (for example, *K84*) were ignored in evaluating the ratio in Figure 1B. The results demonstrated that the expressions of *K4*, *K13*, *K15*, *K76* (formerly known as *K2b*) and *K78* (*K5b*) were significantly downregulated in the OSCC cells, while those of *K6b*, *K10*, *K14*, *K16*, *K17* and *K75* (*K6hf*) were upregulated. The

downregulation of K4 or K13 was observed in most cases (Figure 1C). Although many studies have reported upregulation of K8 and K18 during oral carcinogenesis<sup>5, 6, 11, 16, 21, 22</sup>, OSCC cases with elevated expression of K8, K18 were exceptional and their expression levels were low compared to those of the other keratins (data not shown and Figure 1D). In contrast, significant upregulation of K17 was observed in most cases (Figure 1D).

Identification of the keratins with altered expression patterns in oral neoplastic lesions  
 Since the microarray data revealed complex variations in the expression of the different keratin subtypes, we attempted to thoroughly examine their expression patterns at a histological level. Considering that oral epithelium shows diverse appearances depending on the site, we first examined the keratin expression profile in normal oral epithelium including tongue, gingiva, buccal mucosa and oral floor. Keratin expression profiles were basically the same throughout the oral cavity. K4 and K13 were strongly expressed in suprabasal cells, whereas in the basal cells, K5, K14, K15 and K19 were expressed. K6 and K16 were also expressed weakly in the suprabasal layer. Parts of the gingiva, palate and tongue papilla that are sites of masticatory mucosa showed a different expression pattern, where K4 and K13 expression was weakly detected in dispersed cells and K1 and K10 were expressed instead. Next we collected 10 cases of OSCC associated with OED in the tongue, gingiva, buccal mucosa and oral floor and investigated the expression of the keratins. A panel of keratin expression in a representative case is presented

in the Supporting Information. K4 and K13 were significantly downregulated or almost disappeared in OSCC and OED. K17, which was negative or faintly detected in normal mucosa, was upregulated in the basal and suprabasal layer of most cases. K1 and K10 were also considerably upregulated in the suprabasal layers of more than half of OSCC and OED cases. K6 and K16 were diffusely upregulated in OSCC and also in OED of 6 cases. K2 was negative in normal mucosa but was detected in dispersed cells of 2 cases. K5 and K14 showed no alteration of expression in the basal cells, while the expression retained in the suprabasal cells of OED and was detected in virtually all the OSCC cells. The expression of K15 and K19 showed various alterations in OSCC and OED: both were exclusively expressed in the basal cells of normal epithelium, but the expression frequently disappeared in OED, either completely or in dispersed cells. In OSCC, K15 and K19 were either completely negative or were detected diffusely or in dispersed cells. The summary of the immunohistochemical findings is schematically represented in Figure 2A. Overall alteration of keratin expression revealed by microarray array analysis and immunohistochemistry is also depicted schematically on a genome map (Figure 2B). These results confirmed the microarray data and highlighted relevant keratins to distinguish OED and OSCC from a normal epithelium. Among these, the downregulation of K4 and K13 expression in lining mucosa was the most consistent and apparent. In contrast, expression of the other keratins showed various case-dependent alterations. K4 and K13 are a dominant and specific pair in suprabasal cells

of oral lining mucosa, and represent their terminal differentiation. Therefore, we focused on K4 and K13 expression in further experiments.

K4 and K13 expression is consistently downregulated in OSCC and OED

To further investigate the expression of K4 and K13 in OSCC and OED, we performed immunohistochemical examination of an additional 90 cases (40 OSCCs and 50 OEDs) (Figure 3). K4 expression was aberrant in all cases of OSCC and OED. K13 expression was aberrant in all cases of OSCC except one case of very well-differentiated SCC, and in 70% (35/50) cases of OED. The downregulation of these proteins was a result of an increase in the number of cells with complete loss of K4 and K13 expression, and not a result of reduction of expression in individual cells. Loss of K4 and K13 expression usually occurred concomitantly, but K4(-) cells were often distributed more broadly in the lesions compared to K13(-) cells (Figure 3A, B). This suggests that the expression of K4 represents the terminal differentiation of oral keratinocytes more strictly than K13, and thus can be used as a more sensitive indicator for its dysregulation. In the OSCC lesions, most of the cancer cells were negative for both K4 and K13 expression (Figure 3A, B, C), although cancer nests with dispersed K4- and/or K13-positive cells were occasionally observed (Figure 3A). Using immunohistochemistry we investigated the cases in which a considerably retained level of K4 or/and K13 expression was indicated by the microarray analysis (marked with '+' or '#' respectively in Figure 1C), and confirmed that they also showed significant downregulation of

K4 and K13. This minor inconsistency between the microarray analysis and the immunohistochemical examination was apparently due to the sampling from the lesions in which K13-positive (and a few K4-positive) and K13-negative cancer nests coexisted.

In OED, K4 expression was absent or significantly downregulated in all cases (Figure 3D). Both leukoplakic and erythroplakic lesions showed aberrant K4 expression, regardless of the grade of OED (Figure 3C, D). K13 was also significantly downregulated in 6 out of 16 cases of mild OED, 19 out of 24 cases of moderate OED and all the cases of severe OED. A prominent feature in this observation was that aberrant K4 expression was always observed in a region that exhibited abnormal morphology (dysplasia) and was not observed in epithelium with normal appearance. Since the adjacent epithelium usually showed normal K4 expression, the borders of K4 expression were clearly visible. Because of these features, a dysplastic lesion could be distinguished from a normal epithelium by examining the K4 expression. At the periphery of the lesion, the distribution of K4(-) cells could be divided into 2 patterns.

Type 1: In a majority of the cases (38/60), a definite border between the K4 positive and negative regions was observed. The border of K13 expression matched that of K4 expression, although some K13(+) cells often remained in the K4(-) region. In this category, a clear histological demarcation between the normal epithelium and OED was visible, and the histological border coincided with the K4 expression border.

Type 2: In a smaller number of cases (22/60), there was a gradual increase in the number of

K4(-) cells towards the center of the lesion, forming a transient zone with a mixed population of K4-positive and negative cells. In these cases, no distinct histological border was visible.

We examined the coexpression of K4 and K13 in individual cells by immunofluorescent double staining in 10 representative cases of OED. In the normal oral mucosa, suprabasal cells coexpressed both K4 and K13 (Figure 4A). In cases with Type 1 borders, K4(-)K13(-) cells were predominantly observed in the lesion with very few K4(-)K13(+) cells (Figure 4B). In the cases with Type 2 borders, the transient zones comprising mixed populations of K4(+)K13(+), K4(-)K13(-), and K4(-)K13(+) cells were observed. In addition, a few cells with K4(+)K13(-) phenotype, which were never observed in the normal epithelia, were observed (Figure 4C).

#### Pathophysiological role of altered keratin expression

Since the loss of K4 expression was highly correlated with the presence of OED, we hypothesized that aberrant expression of K4 and K13, as well as concomitant upregulation of the other keratins, may be one of the causes of OED. To check this hypothesis, we transfected *K4*, *dnK4*, and *K13* in Ca9-22 cells. The keratins were tagged with GFP (K4; green) or RFP (K13; red), allowing direct visualization of keratin filaments. DnK4 could form aggregates with a broad range of keratin subtypes, causing impaired keratin network formation (data not shown). Cotransfection of cognate keratin subtypes (i.e., *K4* and *K13*) resulted in a filamentous arrangement of each keratin subtype (Figure 5A). In contrast,

cotransfection of *dnK4* with *K13* resulted in the aggregation of both the keratin subtypes, and the dnK4-expressing cells decreased in size, were round, and showed poor adhesion to the surrounding cells (Figure 5A). These results implied that the impaired formation of a keratin network resulted in alteration in cell shape and attachment. We next investigated whether K4 or K13 is functional in the absence of its cognate partner. To address this issue, we used the osteosarcoma cell line U2OS because no keratins were expressed in this cell line (data not shown). We first transfected U2OS cells with the genes of the following keratin subtypes: *K4*, *K5*, *K13*, and *K14*; we then examined the distribution of each keratin subtype. As shown in Figure 5B, basic keratins (K4 and K5) exhibited a filamentous network, whereas acidic keratins (K13 and K14) exhibited a diffuse distribution and lacked a filamentous network. This finding suggested that K13 and K14 were not functional in the absence of the basic keratins, although K4 and K5 were somehow integrated into the cytoskeletal network of the U2OS cells. These results suggested that aberrant expression of only one keratin subtype could cause an impaired cytoskeletal network. Nevertheless, a majority of the cells in OED retain relatively normal cytomorphology in the absence of K4 or K13 expression. We assumed that the other keratin subtypes that were ectopically induced could compensate for the loss of K4 or K13. To check this hypothesis, we cotransfected the U2OS cells with different pairs of these keratins to investigate the mutual interaction of each keratin in the cytoskeletal network formation. Cotransfection with any of the combinations of keratin subtypes, that is,

K4/K13 (a cognate pair of differentiation-related keratins), K5/K14 (a cognate pair of basal cell keratins), K4/K14 and K5/K13, resulted in the formation of similar cytoskeletal network, as observed with the single-gene transfection of K4 or K5 (Figure 5B). This suggested that K5 and K14 could compensate for the function of K4 and K13, respectively, in the cytoskeletal network formation. Finally, we examined the effect of keratin subtype expression on cell movement using a Boyden chamber assay. K17-transfected cells showed increased motility compared to mock- or K13-transfected cells (Figure 5C). This result implies that induction of K17 expression, which occurs in most cases of OSCC and OED, may lead to architectural alteration of the epithelium due to increased cell movement. Taking these results together with the *in situ* observations demonstrating that the epithelia with aberrant K4 or/and K13 expression always exhibited morphological alterations, we assume that aberrant expression of these differentiation-related keratins and concomitant upregulation of other keratins may be one of the causative factors for cytological and architectural alteration of the affected epithelium.

### Discussion

We demonstrated that the following features of K4 and K13 render them as relevant biomarkers for OED as well as OSCC: (1) Distinct expression in individual cells enables precise and reliable evaluation. (2) They were consistently downregulated in OSCC and OED. (3) These keratins are major keratin pairs in the suprabasal cells of oral epithelium, and thus

their aberrant expression indicates abnormal terminal differentiation. Since K4 was more sensitive and was more broadly downregulated in the lesion than K13, we think that K4 is the first choice as a marker for dysregulation of oral epithelial differentiation. We compared the expression of K4 with that of Ki67 and TP53, and found that the usability of K4 was comparable to or even more sensitive than these commonly used markers for malignancy (unpublished data). Combined usage of these markers for different cellular properties would facilitate more precise diagnosis.

OEDs are commonly experienced as a white patch (leukoplakia) or a red lesion (erythroplakia). The former could be roughly divided into two types of lesions in the context of their keratin profiles. The one was a K1(+)K10(+) lesion, in which the expressions of K4 and K13 were substituted for by their epidermal counterparts, K1 and K10, respectively, and the lesion exhibited an orthokeratotic appearance. The other was a K1(-)K10(-) lesion that typically showed hyperparakeratosis, although this keratosis was not achieved by original K4 and K13 pairs, but by the other upregulated keratins such as K5, K6, K14, K16 and especially K17. When little expression of the differentiation-related keratins was induced, the lesion led to poor development of the prickled cell layer, exhibiting an erythroplakic appearance (unpublished data). These are examples of the direct correlation between alteration of keratin expression and changes in the epithelial morphology. In any case, downregulation of K4 and K13 seemed essential since we never observed the other keratins upregulation in the presence of normal expression of K4 and K13.

Missense mutations in either *K4* and *K13* genes can cause white sponge nevus (WSN).<sup>23, 24</sup> Furthermore, *K4* knockout mice show the cellular phenotype that resembles epithelial dysplasia in humans, including hyperkeratosis, atypical nuclei, and cell degeneration.<sup>25</sup> Although commonly experienced OED usually showed somewhat different histological features from that of WSN and the *K4*-knockout mice, these imply that aberrant expression of *K4* or *K13* may possibly lead to morphological change of the affected epithelium. In fact, we demonstrated that regions with aberrant *K4* and *K13* expression highly coincided with altered epithelial morphology, including the concurrent formation of a histological border with a *K4*-expression border. Cell culture experiments suggest that aberrant keratin expression and impaired cytoskeletal network formation could cause changes in cell shape. However, this may not be a dominant factor for alteration of the whole epithelial morphology, because other keratins are usually induced so as to compensate for the absence of the original keratins expression. Rather, increased cell motility represented by *K6*, *K16* and *K17* expression may associate with architectural alteration. These keratins are robustly induced in a hyperproliferative epithelium after injury, and their presence correlates with changes in the morphology of epithelial cells at the wound edge.<sup>26</sup> Forced expression of *K16* in progenitor skin keratinocytes directly impacts properties such as adhesion and migration.<sup>27</sup> Furthermore, our results demonstrated that forced expression of *K17* led to increased cell migration. Altogether, we assume that alteration of keratin subtype expression is one of the factors that

underlie cytological and architectural alterations observed in OED and OSCC. If so, keratin profiling is not only a practical but also a rational aid for pathological diagnosis.

The upstream factors that initiate changes in keratin subtype expression in the oral mucosa are currently unknown. We immunohistochemically examined several factors that reportedly regulate keratinocyte differentiation, such as p63, FoxN1, AKT, ERK, FAK and integrins, but none showed a correlation with *K4* and *K13* expression (data not shown). A high correlation between *K4* and *K13* expression patterns suggests the presence of a common mechanism to regulate their transcription, but little sequence homology was found in their promoter regions (data not shown). The well-coordinated regulation of multiple keratin expression may be associated with the unique genome organization of keratin genes. Basic and acidic keratin genes, except *K18* (which locates on *12q* back to back with *K8*), are tandemly aligned on *12q* and *17q*, respectively, and this genomic organization is evolutionary well-conserved. Our comprehensive keratin profiling revealed that each of the upregulated and downregulated keratins in OSCC and OED was seemingly clustered on the genome (Figure 2B). This implicated that the epigenetic status of keratin loci may be important for the selective expression of specific repertoires of keratins. In this sense, analysis of methylation states in the keratin loci would be an interesting future project for understanding the coordinated expression of different keratin subtypes. In conclusion, our study demonstrated that aberrant expression of *K4* and *K13*, which are differentiation-related keratins in oral

keratinocytes, was the most essential feature observed in OSCC and OED.

### Acknowledgments

This work was supported by a grant-in-aid from the Japanese Ministry of Education, Culture, Sports, Science and Technology (KAKENHI 21592320). The authors thank Miwako Hamagaki and Kiyoko Nagumo for technical assistance and undergraduate students Yuhei Ikeda and Ryushiro Sugita for their contributions to this study.

### References

1. Moll R, Divo M, Langbein L. The human keratins: biology and pathology. *Histochem Cell Biol* 2008;**129**:705-733.
2. Crowe DL, Milo GE, Shuler CF. Keratin 19 downregulation by oral squamous cell carcinoma lines increases invasive potential. *J Dent Res* 1999;**78**:1256-1263.
3. Farrar M, Sandison A, Peston D, Gailani M. Immunocytochemical analysis of AE1/AE3, CK 14, Ki-67 and p53 expression in benign, premalignant and malignant oral tissue to establish putative markers for progression of oral carcinoma. *Br J Biomed Sci* 2004;**61**:117-124.
4. Fillies T, Werkmeister R, Packeisen J *et al*. Cytokeratin 8/18 expression indicates a poor prognosis in squamous cell carcinomas of the oral cavity. *BMC Cancer* 2006;**6**:10.
5. Gires O, Mack B, Rauch J, Matthias C. CK8 correlates with malignancy in leukoplakia and carcinomas of the head and neck. *Biochem Biophys Res Commun* 2006;**343**:252-259.
6. Matthias C, Mack B, Berghaus A, Gires O. Keratin 8 expression in head and neck epithelia. *BMC Cancer* 2008;**8**:267.
7. Ogden GR, Lane EB, Hopwood DV, Chisholm DM. Evidence for field change in oral cancer based on cytokeratin expression. *Br J Cancer* 1993;**67**:1324-1330.
8. Ohkura S, Kondoh N, Hada A *et al*. Differential expression of the keratin-4, -13, -14, -17 and transglutaminase 3 genes during the development of oral squamous cell carcinoma from leukoplakia. *Oral Oncol* 2005;**41**:607-613.
9. Su L, Morgan PR, Lane EB. Keratin 14 and 19 expression in normal, dysplastic and malignant oral epithelia. A study using in situ hybridization and immunohistochemistry. *J Oral Pathol Med* 1996;**25**:293-301.
10. Toyoshima T, Vairaktaris E, Nkenke E, Schlegel KA, Neukam FW, Ries J. Cytokeratin 17 mRNA expression has potential for diagnostic marker of oral squamous cell carcinoma. *J Cancer Res Clin Oncol* 2008;**134**:515-521.
11. Xu XC, Lee JS, Lippman SM, Ro JY, Hong WK, Lotan R. Increased expression of cytokeratins CK8 and CK19 is associated with head and neck carcinogenesis. *Cancer Epidemiol Biomarkers Prev* 1995;**4**:871-876.
12. Yanagawa T, Yoshida H, Yamagata K *et al*. Loss of cytokeratin 13 expression in squamous cell carcinoma of the tongue is a possible sign for local recurrence. *J Exp Clin Cancer Res* 2007;**26**:215-220.
13. Zhong LP, Chen WT, Zhang CP, Zhang ZY. Increased CK19 expression correlated with pathologic differentiation grade and prognosis in oral squamous cell carcinoma patients. *Oral Surg Oral Med Oral Pathol Oral Radiol Endod* 2007;**104**:377-384.
14. Depondt J, Shabana AH, Sawaf H, Gehanno P, Forest N. Cytokeratin alterations as diagnostic and prognostic markers of oral and

- pharyngeal carcinomas. A prospective study. *Eur J Oral Sci* 1999;**107**;442-454.
15. Fillies T, Jogschies M, Kleinheinz J, Brandt B, Joos U, Buerger H. Cytokeratin alteration in oral leukoplakia and oral squamous cell carcinoma. *Oncol Rep* 2007;**18**;639-643.
16. Ogden GR, Chisholm DM, Adi M, Lane EB. Cytokeratin expression in oral cancer and its relationship to tumor differentiation. *J Oral Pathol Med* 1993;**22**;82-86.
17. Vaidya MM, Borges AM, Pradhan SA, Bhisey AN. Cytokeratin expression in squamous cell carcinomas of the tongue and alveolar mucosa. *Eur J Cancer B Oral Oncol* 1996;**32B**;333-336.
18. Barnes L, Eveson J, Reichart P, Sidransky D. Epithelial precursor lesions. *World Health Organization Classification of Tumours. Pathology & genetics. Head and neck tumours* 2005;177-180.
19. Tomioka H, Morita K, Hasegawa S, Omura K. Gene expression analysis by cDNA microarray in oral squamous cell carcinoma. *J Oral Pathol Med* 2006;**35**;206-211.
20. Bonifacino JS, Dasso M, Harford JB, Lippincott-Schwartz J, Yamada KM. *Current Protocols in Cell Biology*: John Wiley and Sons, Inc., 2007.
21. Su L, Morgan PR, Lane EB. Protein and mRNA expression of simple epithelial keratins in normal, dysplastic, and malignant oral epithelia. *Am J Pathol* 1994;**145**;1349-1357.
22. Zhong LP, Zhao SF, Chen GF, Ping FY, Xu ZF, Hu JA. Increased levels of CK19 mRNA in oral squamous cell carcinoma tissue detected by relative quantification with real-time polymerase chain reaction. *Arch Oral Biol* 2006;**51**;1112-1119.
23. Richard G, De Laurenzi V, Didona B, Bale SJ, Compton JG. Keratin 13 point mutation underlies the hereditary mucosal epithelial disorder white sponge nevus. *Nat Genet* 1995;**11**;453-455.
24. Rugg EL, McLean WH, Allison WE *et al*. A mutation in the mucosal keratin K4 is associated with oral white sponge nevus. *Nat Genet* 1995;**11**;450-452.
25. Ness SL, Edelmann W, Jenkins TD, Liedtke W, Rustgi AK, Kucherlapati R. Mouse keratin 4 is necessary for internal epithelial integrity. *J Biol Chem* 1998;**273**;23904-23911.
26. Mazzalupo S, Wong P, Martin P, Coulombe PA. Role for keratins 6 and 17 during wound closure in embryonic mouse skin. *Dev Dyn* 2003;**226**;356-365.
27. Wawersik M, Coulombe PA. Forced expression of keratin 16 alters the adhesion, differentiation, and migration of mouse skin keratinocytes. *Mol Biol Cell* 2000;**11**;3315-3327.



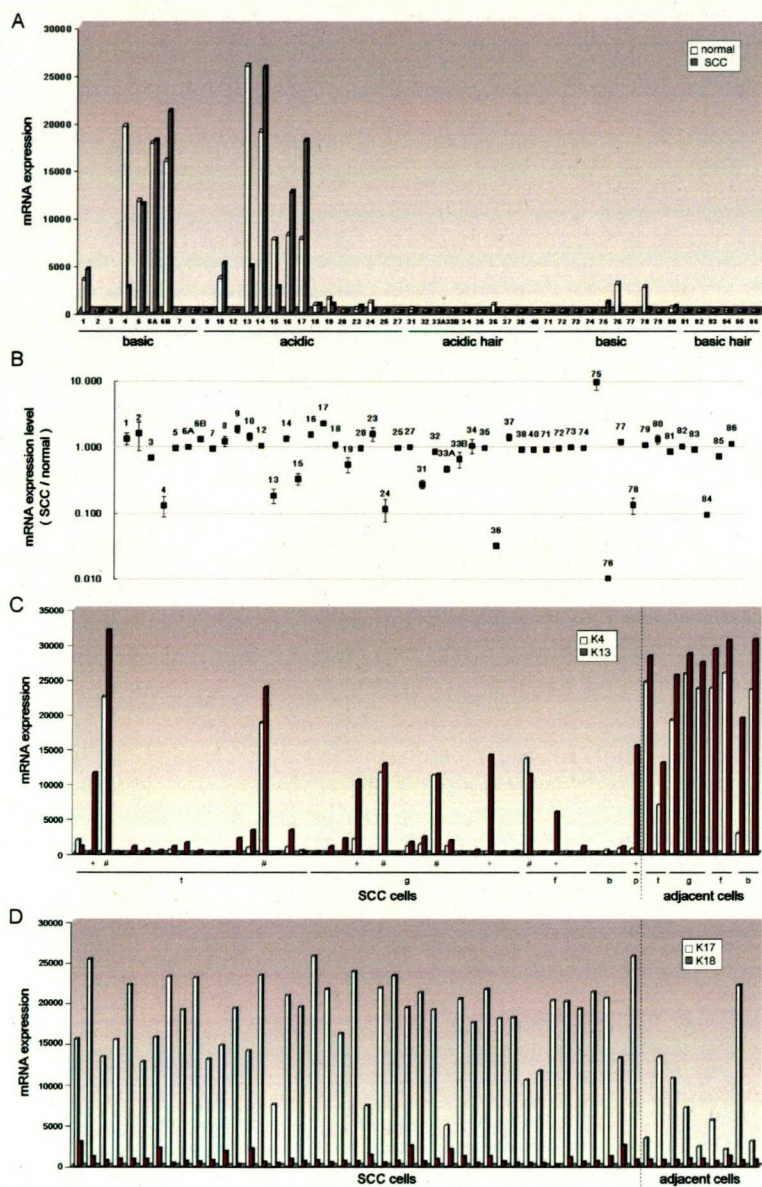


Figure 1. cDNA microarray analysis of oral squamous cell carcinoma (OSCC). A) The expressions of each keratin subtype in 43 OSCC samples and 9 normal control samples are represented as the mean of the fluorescent signal intensity. Numerals in the horizontal axis denote the keratin subtypes. K1–K8 and K71–K80 are basic epithelial keratins. K9–K27 are acidic epithelial keratins. K31–K40 are acidic hair keratins and K81–K86 are basic hair keratins. Expressions of pseudogenes were omitted. B) The expression levels are represented as the ratios of the mean expression in OSCC to that in the normal samples. Error bars denote standard errors. Numerals denote the keratin subtypes. The vertical axis is logarithmic. C) The K4 and K13 signal intensities of each OSCC that arose in tongue (t), gingiva (g), oral floor (f), buccal mucosa (b) and palate (p). Nine samples to the right are the normal control samples. Crosses denote the cases with considerably retained expression of K13 but not K4. Sharps denote the cases with considerably retained expression of both K4 and K13. D) The K17 and K18 signal intensities of each case.  
495x759mm (96 x 96 DPI)

For Peer Review

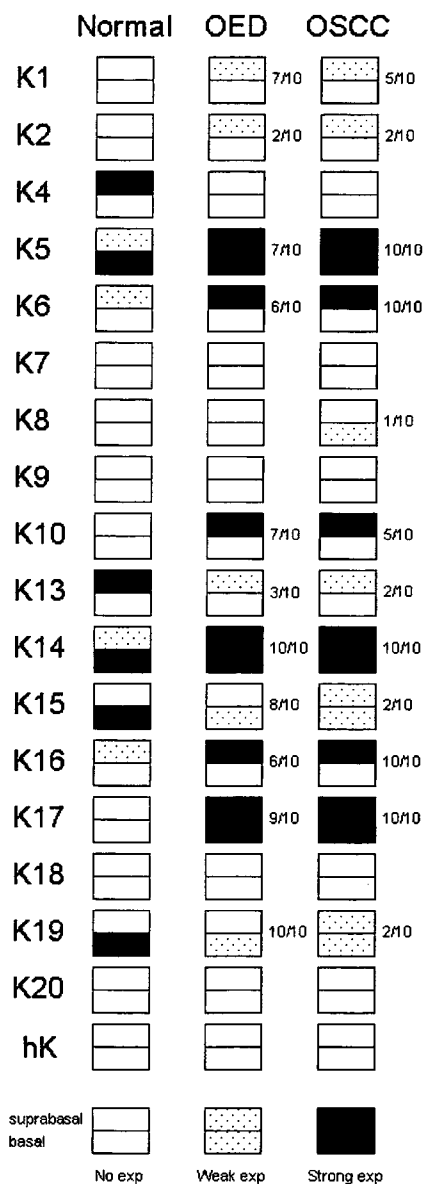


Figure 2A. Schematic illustration of keratin expression profile in the normal oral mucosa, oral epithelial dysplasia (OED) and oral squamous cell carcinoma (OSCC). The epithelium is divided into two compartments – the basal and the suprabasal compartments – and the expression is represented by a 3-grade evaluation. The black shading (strong expression) represents that the expression was observed strongly in virtually all cells in the positive case. The white shading (no expression) represents that the expression was almost completely negative in all the cases. The dotted shading (weak expression) represents that the expression was detected weakly or partially. Number of the cases with an altered expression pattern is also shown.

82x222mm (96 x 96 DPI)

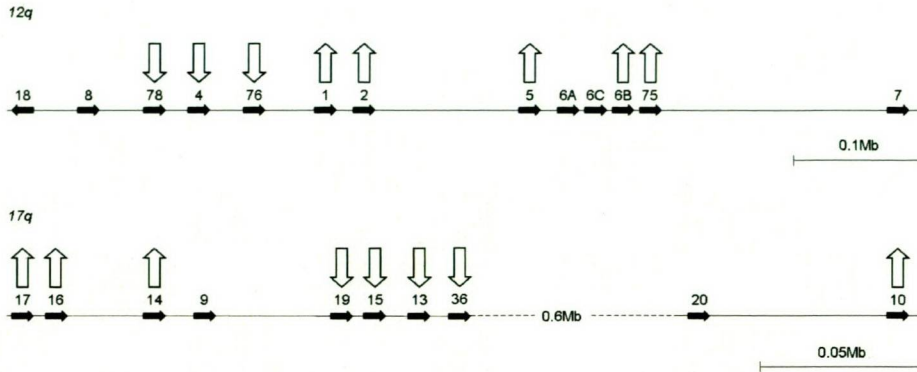


Figure 2B. Schematic illustration of the keratin loci, also showing keratins upregulated (upward arrow) or downregulated (downward arrow) in OSCC and OED. Only major epithelial keratins and keratins that exhibited significant change of expression are depicted. The sizes of the genes are not reproduced in the figure.  
381x190mm (96 x 96 DPI)

Peer Review